

Reactivity of LGe–NR₂ and LGe(E)–NR₂ over LGe–Cl and LGe(E)–Cl toward Me₃SiX (L = Aminotroponimate; NR₂ = N(SiMe₃)₂/NC₄H₄; E = S/Se; X = Br/CN)

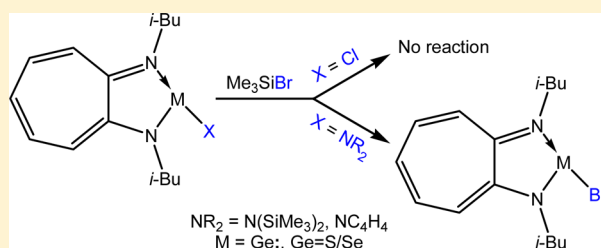
Rahul Kumar Siwath,[†] Surendar Karwasara,[†] Mahendra Kumar Sharma,[†] Santigopal Mondal,[†] Goutam Mukherjee,[†] Gopalan Rajaraman,[‡] and Selvarajan Nagendran^{*,†}

[†]Department of Chemistry, Indian Institute of Technology Delhi, Hauz Khas, New Delhi 110 016, India

[‡]Department of Chemistry, Indian Institute of Technology Bombay, Powai, Mumbai 400 076, India

Supporting Information

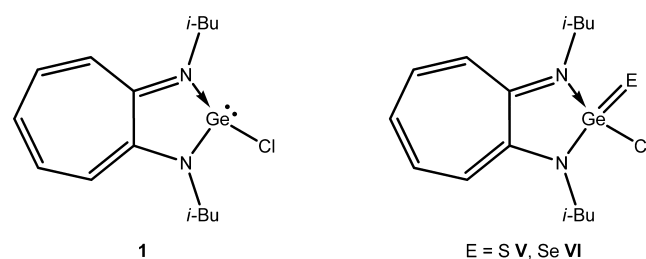
ABSTRACT: The halogen exchange reaction of either germylene monochloride [LGeCl] (1) or germachalcogenoacid chlorides [LGe(E)Cl] (L = (*i*-Bu)₂ATI; ATI = aminotroponimate; E = S (V)/Se (VI)) with Me₃SiX (X = Br/CN) did not occur. Therefore, the reactions of germanium compounds containing Ge–N bonds with Me₃SiBr/CN were tried. Germylene amide [LGeN(SiMe₃)₂] (2) reacted with Me₃SiBr to afford the aminotroponimatogermylene monobromide [LGeBr] (3). Similarly, the chalcogen derivatives of compound 2, viz., germachalcogenoamides [LGe(E)N(SiMe₃)₂] (E = S 4 and Se 5) reacted with Me₃SiBr and resulted in germachalcogenoacid bromides [LGe(E)Br] (E = S 6 and Se 7), respectively. *N*-Germylene pyrrole [LGeNC₄H₄] (2a) and *N*-germachalcogenoacylpyrroles [LGe(E)NC₄H₄] (E = S 4a, Se 5a) also reacted with Me₃SiBr and afforded compounds 3, and 6–7 in excellent yields, respectively. Interestingly, the reaction of compound 2a with Me₃SiCN afforded germanium(II) cyanide [LGeCN] (8). The difference in the reactivity of compounds (1, V, and VI) with Ge–Cl bonds against the compounds (2, 4, and 5) with Ge–N bonds was analyzed theoretically.



INTRODUCTION

Chlorogermynes are the most widely used precursors for the synthesis of other germylene derivatives¹ since the isolation of dichlorogermylene–dioxane complex² (GeCl₂·dioxane). Although, fluoro-,³ bromo-,⁴ and iodogermynes⁵ are reported in the literature, the examples are limited and their reactivity is less explored.¹ The halogen exchange reactions of chlorogermynes with reagents such as Me₃SnF, Me₃SiBr, and Me₃SiI generally result in the fluoro-, bromo-, and iodogermynes, respectively.^{3–5} Isolation of β-diketiminatogermylene monofluoride [HC{C(Me)NAr}₂GeF] (II) (Ar = 2,6-(*i*-Pr)₂C₆H₃) through the reaction of [HC{C(Me)NAr}₂GeCl] (I) with Me₃SnF was reported by Roesky and co-workers.^{3c} Baines and co-workers carried out the reactions of NHC-stabilized germanium(II) dichloride complexes [NHC→GeCl₂] (NHC = {C(Me)N(R¹)₂C:} (R¹ = Me or *i*-Pr) with Me₃SiBr and Me₃SiI to get [NHC→GeBr₂] and [NHC→GeI₂] complexes, respectively.^{4c,d,5a} Further, as reported by Castel and co-workers, the amidinatogermylene monochloride [PhC(NSiMe₃)₂GeCl] (III) also reacted with Me₃SiBr and afforded [PhC(NSiMe₃)₂GeBr] (IV).^{4a} In view of these reports, we anticipated that the aminotroponimatogermylene monochloride^{3b} [(*i*-Bu)₂ATIGeCl] (1) (Chart 1) will also react with Me₃SiBr; nevertheless, no reactivity was observed, surprisingly. Further, the sulfur and selenium derivatives of compound 1, [LGe(S)Cl] (V) and [LGe(Se)Cl] (VI) (L = (*i*-Bu)₂ATI) (Chart 1),^{3b} also did not react with Me₃SiBr.

Chart 1. Structure of Germylene Monochloride 1 and Its Chalcogen Derivatives V and VI

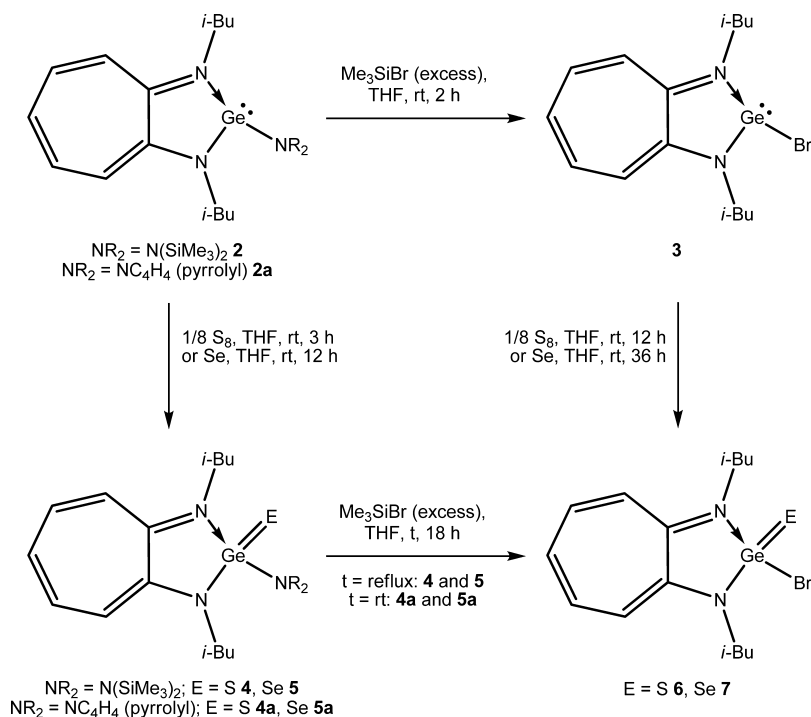


However, we found that germylene amide^{6a} [LGeN(SiMe₃)₂] (2) and *N*-germylenepyrrole^{6b} (2a) react smoothly with Me₃SiBr to afford the germylene monobromide [LGeBr] (3). The products of oxidation of compounds 2 and 2a, namely, germachalcogenoamides [LGe(E)NR₂] (NR₂ = N(SiMe₃)₂; E = S 4, Se 5 and NR₂ = NC₄H₄; E = S 4a, Se 5a) also react with Me₃SiBr to give germachalcogenoacid bromides [LGe(S)Br] (6) and [LGe(Se)Br] (7), which were anticipated from compounds V and VI, respectively. Further, the reaction of compound 2a with other trimethylsilyl group containing reagents, such as Me₃SiCN, occurred easily to give germanium(II) cyanide (8). Accordingly, we demonstrate the utility of

Received: July 27, 2015

Published: February 2, 2016

Scheme 1. Reaction of Compounds 2, 2a, 4, 5, 4a, and 5a with Trimethylsilyl Bromide



compounds with $\text{Ge}^{\text{II}}-\text{NR}_2$ and $(\text{E})\text{Ge}^{\text{IV}}-\text{NR}_2$ bonds ($\text{NR}_2 = \text{N}(\text{SiMe}_3)_2/\text{NC}_4\text{H}_4$; E = S/Se) as useful starting materials for the isolation of other germanium derivatives, where the conventional starting materials such as chlorogermylene and germachalcogenoacid chlorides have failed.

RESULTS AND DISCUSSION

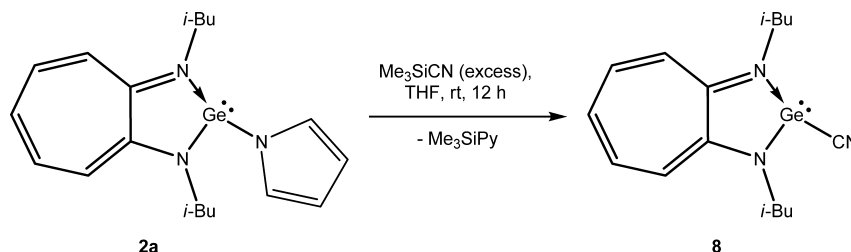
Synthesis and Spectra. While probing the reactivity of aminotroponiminatogermylene monochloride $[\text{LGeCl}]$ (**1**),^{3b} it was noted that compound **1** does not react with Me_3SiBr , which is in contrast to the literature reports, where several germanium(II) chlorides underwent halogen exchange reaction with Me_3SiBr and afforded the corresponding germanium(II) bromides.⁴ Thus, the reactions of compound **1** with excess Me_3SiBr in tetrahydrofuran (or toluene) at room temperature did not give the desired germylene monobromide $[\text{LGeBr}]$ (**3**). Heating these reaction mixtures up to the reflux temperature in tetrahydrofuran or 70 °C in toluene was also not useful. Therefore, other functionalized germylenes, such as germylene amide^{6a} $[\text{LGeN}(\text{SiMe}_3)_2]$ (**2**) obtained by the reaction of compound **1** with lithium bis(trimethylsilyl)amide in hexane at -40 °C, were treated with Me_3SiBr . The reaction of compound **2** at room temperature with an excess of Me_3SiBr in tetrahydrofuran for 2 h afforded germylene monobromide **3** as an orange solid in 97% yield (Scheme 1). Higher bond dissociation enthalpy (BDE) of the Ge–Cl bond and larger HOMO–LUMO energy gap in compound **1** in comparison to the BDE of the Ge–N bond and HOMO–LUMO energy gap in compound **2** are anticipated as the reasons for the lesser reactivity of compound **1** (*vide infra*). As the ATI ligand stabilized germylene amide **2** containing a $\text{Ge}(\text{II})-\text{N}(\text{SiMe}_3)_2$ bond reacted with Me_3SiBr , the feasibility of other $\text{Ge}^{\text{II}}-\text{NR}_2$ bond containing compounds to react with Me_3SiBr was tested. In this direction, the first reaction examined was of *N*-germylenepyrrole $[\text{LGeNC}_4\text{H}_4]$ (**2a**)^{6b} with Me_3SiBr under similar reaction conditions (see the Supporting Information).

Interestingly, compound **2a** also reacts with Me_3SiBr smoothly to give germylene monobromide **3** in 96% yield (Scheme 1). Isolation of compound **3** from compounds **2** and **2a** represents a unique conversion of germylenes with a $\text{Ge}^{\text{II}}-\text{NR}_2$ bond ($\text{NR}_2 = \text{N}(\text{SiMe}_3)_2/\text{NC}_4\text{H}_4$) to germylene monobromide, since an equimolar reaction of the lithium salt of ATI ligand $[(i\text{-Bu})_2\text{ATiLi}(\text{THF})_2]$ with the commercially available GeBr_2 was not clean and resulted in a mixture of germylene monobromide $[\text{LGeBr}]$ (**3**) (64%) and the salt of the ATI ligand $[(i\text{-Bu})_2\text{ATiH}_2]^+[\text{Br}]^-$ (36%) that is not readily separable.

In view of the successful reactions of germanium(II) compounds (**2** and **2a**) with Me_3SiBr , we inquisitively probed the reactions of the oxidative addition products of compounds **2** and **2a** such as $[\text{LGe}(\text{E})\text{NR}_2]$ ($\text{NR}_2 = \text{N}(\text{SiMe}_3)_2$; E = S **4**, Se **5** and $\text{NR}_2 = \text{NC}_4\text{H}_4$; E = S **4a**, Se **5a**)^{6b} containing $(\text{E})\text{Ge}^{\text{IV}}-\text{NR}_2$ bonds with Me_3SiBr . Compounds **4** and **5** were obtained by the reactions of compound **2** with elemental sulfur and selenium at room temperature in tetrahydrofuran (Scheme 1). The reactions of germachalcogenoamides **4** and **5** with an excess of Me_3SiBr in tetrahydrofuran under reflux conditions for 18 h afforded the germathioacid bromide $[\text{LGe}(\text{S})\text{Br}]$ (**6**) and germaselenoacid bromide $[\text{LGe}(\text{Se})\text{Br}]$ (**7**) as yellow and orange solids in good yields (91% and 94%), respectively (Scheme 1). Similarly, compounds $[\text{LGe}(\text{E})\text{NC}_4\text{H}_4]$ (E = S **4a** and Se **5a**)^{6b} also resulted in the germachalcogenoacid bromides **6** and **7** in 94% and 88% yields (see the Supporting Information) upon their reactions with excess Me_3SiBr at room temperature, respectively (Scheme 1). In all these reactions, an excess of Me_3SiBr is found to be essential for the complete conversion of reactants to products.

The reactions resulting in compounds **6** (E = S) and **7** (E = Se) illustrate the hitherto unknown reactivity of $(\text{E})\text{Ge}^{\text{IV}}-\text{NR}_2$ bonded compounds with Me_3SiX (X = a halogen atom). Another interesting and important aspect to be mentioned here is that, although germachalcogenoacid chlorides^{3b} $[\text{LGe}(\text{E})\text{Cl}]$ (E = S **V** and Se **VI**) do not react with Me_3SiBr to give the

Scheme 2. Reaction of Compound 2a with Trimethylsilyl Cyanide



corresponding germachalcogenoacid bromides **6** and **7**, alternatively, these compounds (**6** and **7**) can also be obtained through the direct reactions of germylene bromide **3** with elemental sulfur and selenium, respectively (Scheme 1). Further, to know the reactivity of these Ge–N bond containing compounds toward other trimethylsilyl group containing reagents, the reactions of compounds **2/2a** and **4/5** were carried out with $\text{Me}_3\text{SiI}/\text{Me}_3\text{SiCN}$. The reactions of compound **2** and its chalcogen derivatives ($\text{E} = \text{S}$ **4** and $\text{E} = \text{Se}$ **5**) with Me_3SiI in tetrahydrofuran gave mainly the salt $[(i\text{-Bu})_2\text{ATI}(\text{H}_2)]^+[\text{I}]^-$ of the ATI ligand and a mixture of unidentified products, respectively. The proton source for the formation of a salt in the reaction of compound **2** with Me_3SiI is anticipated to be the tetrahydrofuran used as solvent. Nevertheless, compound **2a** reacts smoothly with Me_3SiCN to give the corresponding germanium(II) cyanide (**8**). Thus, reaction of compound **2a** with an excess of Me_3SiCN in tetrahydrofuran at room temperature afforded germylene monocyanide **8** as an orange solid in excellent yield (96%) (Scheme 2). Since compound **1** was found to be inert towards Me_3SiCN , isolation of compound **8** through the reaction of compound **2a** with Me_3SiCN gains much importance.

In the solid state, compound **2** decomposes slowly at room temperature. Therefore, it has to be stored under low temperature in an inert atmosphere of nitrogen or argon. Nevertheless, when dissolved in organic solvents, such as hexane, benzene, toluene, and tetrahydrofuran, its solution is very stable at room temperature. However, its solution in a chlorinated solvent decomposes. Other compounds (**3–8**) are stable in an inert atmosphere at room temperature for a long period of time, and all of them are soluble in polar organic solvents such as tetrahydrofuran, toluene, chloroform, and dichloromethane.

All these compounds (**2–8**) are characterized in solution by NMR spectroscopic studies. In the ^1H NMR spectrum of germylene amide $[(i\text{-Bu})_2\text{ATI}(\text{GeN}(\text{SiMe}_3)_2)]$ (**2**), the methyl, methine, and diastereotopic methylene protons of the isobutyl substituents resonate as two doublets (0.81 and 1.00 ppm), a multiplet (2.05–2.18 ppm), and two double doublets (3.07 and 3.27 ppm), respectively. The trimethylsilyl protons appear as a sharp singlet at 0.36 ppm. The seven-membered-ring protons resonate as a triplet (6.05 ppm), a doublet (6.14 ppm), and a double doublet (6.63 ppm). The variable temperature (–10 to 60 °C) NMR study in toluene- d_8 showed no change in the splitting pattern/chemical shift and excludes the possibility of inversion at the germanium atom (having a distorted trigonal pyramidal geometry) within this temperature range⁷ (Figure S1; see the Supporting Information). The isobutyl protons in germylene monobromide **3** appear as a doublet, a multiplet, and a doublet at 1.05, 2.20–2.33, and 3.56 ppm, respectively. The seven-membered-ring protons resonate as a triplet (6.83 ppm), doublet (6.93 ppm), and pseudotriplet (7.34 ppm) in a

1:2:2 intensity ratio. In the ^1H NMR spectra of germachalcogenoamides $[\text{LGe}(\text{E})\text{N}(\text{SiMe}_3)_2]$ ($\text{E} = \text{S}$ **4**, Se **5**) and germachalcogenoacid bromides $[\text{LGe}(\text{E})\text{Br}]$ ($\text{E} = \text{S}$ **6**, Se **7**), all the resonances are downfield shifted in comparison to their germanium(II) precursors **2** and **3**, respectively. Thus, the protons of methyl, methine, and diastereotopic methylene groups of the isobutyl substituents in compounds **4–7** resonate as two doublets (in compounds **4**, **5**, and **7**)/one doublet (in compound **6**) (1.06–1.12 ppm), a multiplet (2.36–2.56 ppm), and two double doublets (3.04–3.84 ppm), respectively. The resonance pattern seen for the five seven-membered-ring protons in compound **3** is also observed in the spectra of compounds **4–7** in the region from 6.77 to 7.56 ppm. The trimethylsilyl protons in compounds **4** and **5** resonate as sharp singlets at 0.24 and 0.27 ppm, respectively. In compound **8**, the methyl, methine, and methylene protons of the isobutyl substituents appear as a doublet (1.04 ppm), multiplet (2.12–2.26 ppm), and two double doublets (3.29 and 3.40 ppm), respectively. The seven-membered-ring protons resonate between 6.58 and 7.18 ppm. In the ^{13}C NMR spectra of these compounds, a total of seven (compound **3**), nine (compounds **2**, **4**, and **5**), eight (compounds **6** and **7**), and nine (compound **8**) resonances are seen. In compounds **2** and **4–8**, an additional signal than the expectation is due to the appearance of methyl carbon of the isobutyl substituents as two signals. In compounds **2**, **4**, and **5**, a resonance for the trimethylsilyl carbon atoms is observed as anticipated (5.78–6.08 ppm). The resonance for the carbon atom of the cyanide group in compound **8** appeared at 137.48 ppm and is close to the same resonance (139.19 ppm) found in germylene monocyanide $[(i\text{-Bu})_2\text{ATI}(\text{GeCN})]$ (**IX**).⁸ A medium band at 2124 cm^{-1} in the IR spectrum of compound **8** additionally confirms the presence of a CN group. In the ^{29}Si NMR spectra of compounds **2**, **4**, and **5**, signals at –0.93, 5.36, and 5.56 ppm are suggestive of the presence of trimethylsilyl groups, respectively. In the ^{77}Se NMR spectra of compounds **5** and **7**, the resonances for the selenium atoms in the Ge=Se bonds appear at –183.31 and –128.15 ppm, respectively, and are comparable to the same resonances found in other Ge=Se bond containing compounds stabilized through ATI ligands.^{3b,6b,9} The UV–vis spectra of compounds **3**, **6**, and **7** show two, one, and one absorption maxima in the visible region, respectively (Figure 1). On the basis of theoretical studies, it is predicted that the origins of these peaks in germylene monobromide (**3**) and germachalcogenoacid bromides ($\text{E} = \text{S}$ **6**, Se **7**) are due to the $\pi_{(\text{ATI})} + n_{(\text{Br})} + n_{(\text{Ge})} \rightarrow \pi^*_{(\text{ATI})}$ and $\pi_{(\text{Ge}=\text{E})} + n_{(\text{Br})} \rightarrow \pi^*_{(\text{ATI})}$ electronic transitions, respectively (Table 1). Apart from this, these compounds in common show two intense peaks around 360 and 270 nm (Figure 1) that are due to multiple transitions (Table 1).

X-ray Crystal Structure of Compounds 3–8. Single crystals of compounds **3–8** suitable for X-ray diffraction

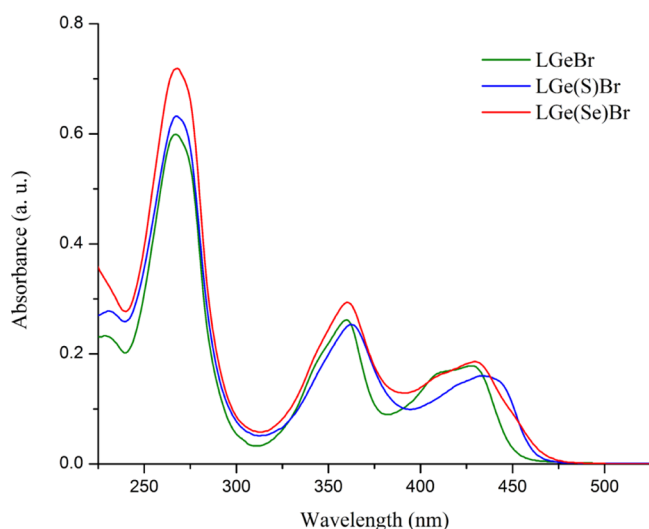


Figure 1. UV-vis spectra of LGeBr (**3**), LGe(S)Br (**6**), and LGe(Se)Br (**7**) (16.7 μ M solution) in tetrahydrofuran.

analysis were grown by either cooling or slow evaporation of their tetrahydrofuran solutions (see the [Experimental Section](#) and the [Supporting Information](#) for details). Compounds **3**, **4/5**, **6/7**, and **8** crystallized in the monoclinic, monoclinic, orthorhombic, and monoclinic space groups $[P2_1/c]$, $[P2_1/n]$, $[Pbca]$, and $[P2_1/c]$, respectively (see Table S1 in the [Supporting Information](#)). Germylene monobromide **3** is monomeric in its solid state and contains a chelating ATI ligand with both the isobutyl substituents oriented opposite to the Ge–Br bond ([Figure 2](#)). The germanium atom possesses two nitrogen atoms of the ATI ligand and a bromine atom in its immediate coordination environment. Therefore, the geometry around the germanium atom is distorted trigonal pyramidal, and the sum of the bond angles is 274.6° . Interestingly, the Ge–Br bond length (2.5324(7) Å) in compound **3** is the longest among the known germylene bromides.⁴ The Ge–Br bond lengths in the reported germylene bromides lie between 2.4239 and 2.5064 Å.⁴ The average Ge–N bond length in compound **3** (1.931 Å) is comparable to the corresponding average in compound **1** (1.938 Å).^{3b}

The molecular structures of germachalcogenoamides [LGe(E)N(SiMe₃)₂] (E = S **4**, [Figure S2](#), see the [Supporting Information](#); and E = Se **5**, [Figure 3](#)) and germachalcogenoacid bromides [LGe(E)Br] (E = S **6**, [Figure 4](#); and E = Se **7**, [Figure S3](#); see the [Supporting Information](#)) show tetracoordinate germanium atoms with distorted tetrahedral geometries. The immediate environments around the germanium atoms in these compounds (**4–7**) contain two nitrogen atoms of the ATI ligand, a chalcogen atom (E = S **4** and **6**, Se **5** and **7**), and a nitrogen atom of the amide group (**4** and **5**)/a bromine atom (**6** and **7**).

The bond lengths of the terminal Ge=S bonds in germathioamide **4** and germathioacid bromide **6** are 2.083(1) and 2.0608(8) Å, respectively. These values match the corresponding bond lengths in germathioester [LGe(S)Ot-Bu] (2.080(2) Å)^{9b} and germathioacid chloride [LGe(S)Cl] (**V**) (2.065(1) Å),^{3b} respectively. Similarly, the terminal Ge=Se bond lengths in germaselenoamide **5** (2.222(1) Å) and germaselenoacid bromide **7** (2.1940(5) Å) are in good agreement with the lengths of the same bonds found in germaselenoester [LGe(Se)Ot-Bu] (2.218(1) Å)^{9b} and germa-

selenoacid chloride [LGe(Se)Cl] (**VI**) (2.190(1) Å),^{3b} respectively. Further, the Ge=S and Ge=Se bond lengths in these compounds (**4–7**) match the lengths of the same bonds in other related compounds.^{1,6b,9–11} However, the Ge=S and Ge=Se bond lengths in compounds **4–7** are slightly longer than the corresponding bond lengths in the kinetically stabilized Tbt(Tip)Ge=S (2.049(3) Å) and Tbt(Tip)Ge=Se (2.180(2) Å), reported by Okazaki and co-workers (Tbt = 2,4,6-tris(bis(trimethylsilyl)methyl)phenyl; Tip = 2,4,6-tris(isopropyl)phenyl).¹² On the basis of these arguments, compounds **4–7** should possess polarized (or formal) Ge=S and Ge=Se double bonds.^{1,3b,9}

The average Ge–N_{ATI} bond lengths in germachalcogenoamides **4** and **5** are 1.895 and 1.908 Å, respectively, whereas marginally shorter bond lengths are observed for the Ge–N_{amide} bonds [**4**: 1.847(3) Å and **5**: 1.844(5) Å]. In the germachalcogenoacid bromides **6** and **7** the average Ge–N bond lengths are also similar (1.878 and 1.879 Å, respectively). The Ge–Br bond lengths in compounds **6** and **7** are 2.3408(5) and 2.3441(5) Å, respectively. Further, these bond lengths almost match the length of the same bond (2.3861(6) Å) in Weinert's tetravalent germanium bromide [(Me₃SiN)₃GeBr].¹³ In contrast to the Ge–N (1.931 Å) (average) and Ge–Br (2.5324(7) Å) bond lengths in germylene monobromide **3**, the corresponding bond lengths in compounds **6** and **7** are considerably shorter (*vide supra*). This shortening is due to the increase in the oxidation state of the germanium atoms to +4 (in compounds **6** and **7**) from +2 (in compound **3**).

The molecular structure of germanium(II) cyanide **8** shows a cyanide group and chelating ATI ligand attached to the germanium atom ([Figure 5](#)). The tricoordinate germanium atom has a distorted trigonal-pyramidal geometry and possesses a carbon and two nitrogen atoms in its coordination environment. The average Ge–N bond length (1.947 Å) is slightly shorter than that (1.972 Å) (average) in germylene monocyanide [(*t*-Bu)₂ATIGeCN] (**IX**).⁸ However, the length of the Ge–C bond (2.091(6) Å) is equal to the length (2.092(2) Å) of the same bond in compound **IX**. The C≡N bond (1.145(7) Å) is marginally longer than that in compound **IX** (1.126(3) Å). A bent Ge–C–N moiety (170.7(5)^o) is also reminiscent of the situation found in compound **IX**.⁸

Computational Studies. In order to understand the reactivity difference between the Ge–Cl and Ge–N bonds in compounds **1** and **2**, we calculated the energy gaps ($E_{\text{LUMO}} - E_{\text{HOMO}}$) between the frontier molecular orbitals in these compounds, which are 81.8 and 73.2 kcal/mol, respectively. This explicitly reveals the relatively higher reactivity of compound **2**. Calculated bond dissociation enthalpies of the Ge–Cl bond in compound **1** (77.5 kcal/mol) and the Ge–N bond in compound **2** (52.4 kcal/mol) ([Table S2](#)) further support the reactive nature of compound **2**. Similarly, BDE calculations were carried for the Ge–Cl and Ge–N bonds in compounds **V** (77.1 kcal/mol)–**VI** (76.0 kcal/mol) and **4** (63.1 kcal/mol)–**5** (60.4 kcal/mol), respectively ([Table S2](#)). These values are suggestive of the high reactivity of compounds **4** and **5** (with Ge–N bonds) over the compounds **V** and **VI** (with Ge–Cl bonds) and reminiscent of the situation in compounds **1** and **2**. Thus, these findings explain, why compounds **1**, **V**, and **VI** do not react and compounds **2**, **4**, and **5** react with Me₃SiBr.

To understand the nature of the Ge–Br bonds in compounds **6** (E = S) and **7** (E = Se) with Ge(E)Br moieties and to compare it with the nature of Ge–F and Ge–Cl bonds

Table 1. Observed and Calculated UV–Vis Absorption Maxima of Compounds 3, 6, and 7^a

transition	origin of transition (percentage contribution)	λ_{\max} (ϵ) observed	λ_{\max} (f) calculated
Compound 3			
$\pi_{(\text{ATI})} + \text{nb}_{(\text{Br})} + \text{nb}_{(\text{Ge})} \rightarrow \pi^*_{(\text{ATI})}$	HOMO \rightarrow LUMO (96)	427 (10 700)	398.82 (0.1025)
–	–	418 (10 200)	–
$\text{nb}_{(\text{Br})} \rightarrow \pi^*_{(\text{ATI})}$	HOMO–2 \rightarrow LUMO (5)	360 (15 700)	377.47 (0.2539)
$\pi_{(\text{ATI})} + \text{nb}_{(\text{Br})} + \text{nb}_{(\text{Ge})} \rightarrow \pi^*_{(\text{ATI})} + \sigma^*_{(\text{Ge–Br})}$	HOMO–1 \rightarrow LUMO+1 (3)		
$\pi_{(\text{ATI})} + \text{nb}_{(\text{Br})} + \text{nb}_{(\text{Ge})} \rightarrow \pi^*_{(\text{ATI})} + \sigma^*_{(\text{Ge–Br})}$	HOMO \rightarrow LUMO+1 (91)		
$a_{(1)} + \pi_{(\text{ATI})} \rightarrow \pi^*_{(\text{ATI})} + \sigma^*_{(\text{Ge–Br})}$	HOMO–4 \rightarrow LUMO+1 (8)	267 (35 900)	245.31 (0.4749)
$\text{nb}_{(\text{Ge})} + \text{nb}_{(\text{Br})} + \pi_{(\text{ATI})} \rightarrow \pi^*_{(\text{ATI})}$	HOMO–3 \rightarrow LUMO (29)		
$\text{nb}_{(\text{Br})} \rightarrow \pi^*_{(\text{ATI})}$	HOMO–2 \rightarrow LUMO (17)		
$\pi_{(\text{ATI})} + \text{nb}_{(\text{Br})} + \text{nb}_{(\text{Ge})} \rightarrow \pi^*_{(\text{ATI})} + \sigma^*_{(\text{Ge–Br})}$	HOMO \rightarrow LUMO+1 (3)		
$\pi_{(\text{ATI})} + \text{nb}_{(\text{Br})} + \text{nb}_{(\text{Ge})} \rightarrow \sigma^*_{(\text{ATI})}$	HOMO \rightarrow LUMO+3 (23)		
$\pi_{(\text{ATI})} + \text{nb}_{(\text{Br})} + \text{nb}_{(\text{Ge})} \rightarrow \sigma^*_{(\text{Ge–Br})}$	HOMO \rightarrow LUMO+4 (14)		
Compound 6			
$\pi_{(\text{Ge=S})} + \text{nb}_{(\text{Br})} \rightarrow \pi^*_{(\text{ATI})}$	HOMO \rightarrow LUMO (96)	435 (9580)	386.58 (0.0963)
$\sigma_{(\text{Ge–S})} + \text{nb}_{(\text{Br})} \rightarrow \pi^*_{(\text{ATI})}$	HOMO–3 \rightarrow LUMO (3)	362 (15 200)	370.57 (0.1701)
$\pi_{(\text{Ge=S})} \rightarrow \pi^*_{(\text{ATI})}$	HOMO–1 \rightarrow LUMO+1 (7)		
$\pi_{(\text{Ge=S})} + \text{nb}_{(\text{Br})} \rightarrow \pi^*_{(\text{ATI})}$	HOMO \rightarrow LUMO+1 (86)		
$a_{(1)} + \pi_{(\text{ATI})} \rightarrow \pi^*_{(\text{ATI})}$	HOMO–5 \rightarrow LUMO (9)	268 (37 800)	255.43 (0.6537)
$a_{(1)} + \pi_{(\text{ATI})} \rightarrow \pi^*_{(\text{ATI})}$	HOMO–4 \rightarrow LUMO+1 (5)		
$\sigma_{(\text{Ge–S})} + \text{nb}_{(\text{Br})} \rightarrow \pi^*_{(\text{ATI})}$	HOMO–3 \rightarrow LUMO (73)		
$\pi_{(\text{Ge=S})} + \text{nb}_{(\text{Br})} \rightarrow \pi^*_{(\text{ATI})}$	HOMO \rightarrow LUMO+1 (4)		
Compound 7			
$\pi_{(\text{Ge=Se})} + \text{nb}_{(\text{Br})} \rightarrow \pi^*_{(\text{ATI})}$	HOMO \rightarrow LUMO+1 (91)	429 (11 100)	393.97 (0.0929)
$a_{(2)} + \pi_{(\text{ATI})} \rightarrow \pi^*_{(\text{ATI})}$	HOMO–2 \rightarrow LUMO+1 (5)		
$\sigma_{(\text{Ge–Se})} + \text{nb}_{(\text{Br})} \rightarrow \pi^*_{(\text{ATI})}$	HOMO–3 \rightarrow LUMO (7)	360 (17 600)	347.78 (0.1784)
$a_{(2)} + \pi_{(\text{ATI})} \rightarrow \pi^*_{(\text{ATI})}$	HOMO–2 \rightarrow LUMO+1 (83)		
$\pi_{(\text{Ge=Se})} + \text{nb}_{(\text{Br})} \rightarrow \pi^*_{(\text{ATI})}$	HOMO \rightarrow LUMO+1 (4)		
$\pi_{(\text{Ge=Se})} + \text{nb}_{(\text{Br})} \rightarrow \sigma^*_{(\text{Ge–Se})} + \sigma^*_{(\text{Ge–Br})}$	HOMO \rightarrow LUMO+2 (3)		
$a_{(1)} + \pi_{(\text{ATI})} \rightarrow \pi^*_{(\text{ATI})}$	HOMO–5 \rightarrow LUMO (9)	268 (43 100)	256.47 (0.5720)
$a_{(1)} + \pi_{(\text{ATI})} \rightarrow \pi^*_{(\text{ATI})}$	HOMO–4 \rightarrow LUMO (4)		
$a_{(1)} + \pi_{(\text{ATI})} \rightarrow \pi^*_{(\text{ATI})}$	HOMO–4 \rightarrow LUMO+1 (13)		
$\sigma_{(\text{Ge–Se})} + \text{nb}_{(\text{Br})} \rightarrow \pi^*_{(\text{ATI})}$	HOMO–3 \rightarrow LUMO (62)		
$\sigma_{(\text{Ge–Se})} + \text{nb}_{(\text{Br})} \rightarrow \pi^*_{(\text{ATI})}$	HOMO–3 \rightarrow LUMO+1 (2)		
$a_{(2)} + \pi_{(\text{ATI})} \rightarrow \pi^*_{(\text{ATI})}$	HOMO–2 \rightarrow LUMO+1 (3)		

^a $a_{(1)} = \text{nb}_{(\text{Br})} + \sigma_{(\text{C–C})} + \sigma_{(\text{C–H})}$, $a_{(2)} = \text{nb}_{(\text{Br})} + \sigma_{(\text{C–C})} + \sigma_{(\text{Ge–Se})}$.

present in other germaacid halides [(*t*-Bu)₂ATiGe(E)F] (E = S **VII**, Se **VIII**) and [(*i*-Bu)₂ATiGe(E)Cl] (E = S **V**, Se **VI**)^{3b} with Ge(E)X moieties (X = F/Cl), respectively, DFT calculations were carried out on these compounds using GAUSSIAN 09 programs,¹⁴ and the details are summarized in Table 2. On the basis of the NPA charges on germanium and halogen (X) atoms in the Ge–X bonds in compounds **V–VIII** and **6/7**, the anticipated decreases and increases in the ionicity and Wiberg bond index (WBI) of the Ge–X bonds when the X atom changes from F to Br through Cl are observed, respectively (Table 2). Natural bond order (NBO) second-order perturbation theory analysis^{15,16} on compounds **6** and **7** (Figure 6a (**6**) and b (**7**)) shows only one significant π -type interaction between the filled p-orbital of bromine and vacant sp^x ($x = 6.46$ (**6**), 5.44 (**7**))-hybridized orbital of germanium. To compare this situation with the other Ge–X bonds (X = F,

Cl) in compounds with Ge(E)X moieties (X = F; E = S **VII**, Se **VIII** and X = Cl; E = S **V**, Se **VI**),^{3b} the NBO second-order perturbation theory analysis^{15,16} was extended to these compounds. Similar to those in compounds **6** and **7**, only one significant π -type interaction (Figures S4(a) (**V**) and S4(b) (**VI**)) was found between the germanium and chlorine atoms in compounds **V** and **VI** (see the Supporting Information). In contrast, the Ge–F bond containing compounds **VII** and **VIII** show one strong σ - and two π -interactions (Figure S4c–g (**VII**) and h–l (**VIII**)). This high degree of NBO interactions seen in the Ge–F bond containing compounds is due to the greater charge separation between fluorine and germanium atoms (Table 2).

NBO analysis of Ge=S/Se bonds in compounds **6** and **7** was also performed (Table 3). It revealed that the σ Ge–S bond in compound **6** is formed through the overlap of the

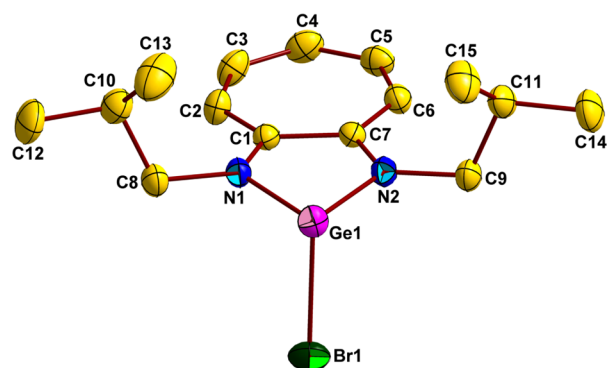


Figure 2. Molecular structure of germylene monobromide **3**. Thermal ellipsoids are drawn at the 25% probability level (data collected at 298(2) K). All the hydrogen atoms are omitted for clarity. Important bond lengths (Å) and angles (deg): Ge1–Br1 2.5324(7), Ge1–N1 1.926(3), Ge1–N2 1.936(3), N1–C1 1.339(4), N2–C7 1.343(4); Br1–Ge1–N1 96.58(9), Br1–Ge1–N2 98.08(8), N1–Ge1–N2 80.0(1).

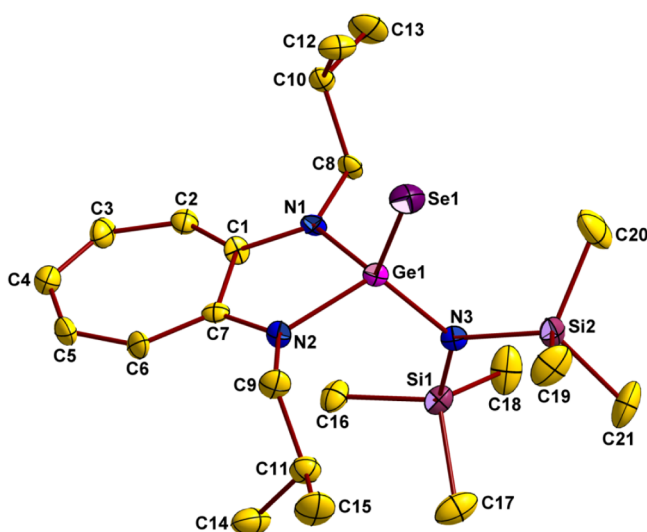


Figure 3. Molecular structure of germselenoamide **5**. Thermal ellipsoids are drawn at the 30% probability level (data collected at 298(2) K). All the hydrogen atoms are omitted for clarity. Important bond lengths (Å) and angles (deg): Ge1–Se1 2.222(1), Ge1–N3 1.844(5), Ge1–N1 1.911(5), Ge1–N2 1.904(5), N1–C1 1.337(8), N2–C7 1.336(8), N3–Si1 1.753(6), N3–Si2 1.776(6); Se1–Ge1–N3 119.7(2), Se1–Ge1–N1 117.5(2), Se1–Ge1–N2 111.0(2), N3–Ge1–N1 108.0(2), N3–Ge1–N2 111.3(2), N1–Ge1–N2 83.7(2), Si1–N3–Si2 119.4(3).

$sp^{0.67}$ -orbital of germanium and the $sp^{6.62}$ -orbital of sulfur with a contribution of 40.6% from germanium and 59.4% from sulfur. The overlap of the $sp^{0.74}$ -orbital of germanium and $sp^{8.02}$ -orbital of selenium resulted in the σ Ge–Se bond in compound **7**. The contribution from germanium and selenium atoms in the σ Ge–Se bond is 45.6% and 54.4%, respectively. The second-order perturbation theory analysis reveals the presence of π -type bonding interactions between germanium and chalcogen atoms in compounds **6** and **7** (Figure 7). In compound **6**, the lateral interaction between the p-orbital of sulfur and the $sp^{6.5}$ -orbital of germanium is stabilized by 13.9 kcal/mol. Similarly in compound **7**, the p-orbital of selenium interacts laterally with the $sp^{5.4}$ -orbital of germanium, which is stabilized by 12.6 kcal/mol. The Wiberg bond indices for the Ge=E (E = S **6**, Se **7**)

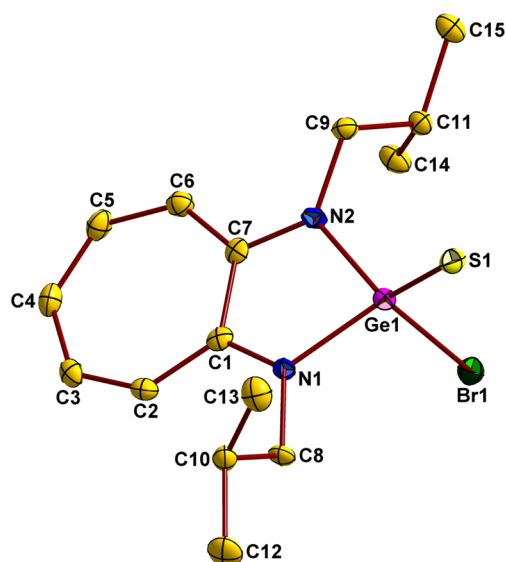


Figure 4. Molecular structure of germathioacid bromide **6**. Thermal ellipsoids are drawn at the 50% probability level (data collected at 100(2) K). All the hydrogen atoms are omitted for clarity. Important bond lengths (Å) and angles (deg): Ge1–S1 2.0608(8), Ge1–Br1 2.3408(5), Ge1–N1 1.876(2), Ge1–N2 1.881(2), N1–C1 1.342(4), N2–C7 1.354(4); S1–Ge1–Br1 113.44(3), S1–Ge1–N1 125.61(7), S1–Ge1–N2 119.89(8), Br1–Ge1–N1 101.01(7), Br1–Ge1–N2 107.81(8), N1–Ge1–N2 84.6(1).

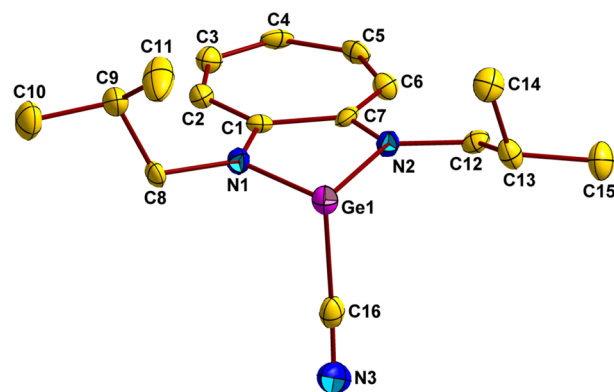


Figure 5. Molecular structure of germylene monocyanide **8**. Thermal ellipsoids are drawn at the 50% probability level (data collected at 150(2) K). All the hydrogen atoms are omitted for clarity. Important bond lengths (Å) and angles (deg): Ge1–C16 2.091(6), C16–N3 1.145(7), Ge1–N1 1.939(4), Ge1–N2 1.955(4), N1–C1 1.345(6), N2–C7 1.348(6); Ge1–C16–N3 170.7(5), C16–Ge1–N1 94.8(2), C16–Ge1–N2 95.2(2), N1–Ge1–N2 80.6(2).

bonds in compounds **6** (1.51) and **7** (1.54) are also suggestive of a formal/polarized double bond between the Ge and E atoms. Moreover, the effect of the lone pair of electrons of the bromine atoms in compounds **6** and **7** on the Ge–E bonds (E = S **6**, Se **7**) was looked at. As Figure 8 reveals, only a marginal interaction was noticed. This is in accordance and in contrast to our earlier findings of the effects the Cl and F atoms have on the Ge–E bonds in compounds V/VI and VII/VIII, respectively.^{3b} Thus, the fluorine lone pairs have greater interactions with the σ -antibonding orbitals of the Ge–E bond as compared to the other halogen atoms in compounds V/VI and **6/7**. Due to this, the Ge=E bond orders are slightly low in the fluorine-containing compounds (Table 3).

Table 2. Computational Data for the Ge–X Bond in Compounds V–VIII, 6, and 7^a

compound	ionicity of the Ge–X bond	WBI of the Ge–X bond	hybridization for Ge–X bond	NPA charges on	
				Ge atom	X atom
L(S)Ge–F (VII)	0.86	0.44	sp ^{4.07} _(Ge) –sp ^{1.92} _(F)	1.92	–0.70
L(Se)Ge–F (VIII)	0.86	0.44	sp ^{4.17} _(Ge) –sp ^{1.91} _(F)	1.82	–0.70
L(S)Ge–Cl (V)	0.70	0.69	sp ^{1.99} _(Ge) –sp ^{4.14} _(Cl)	1.59	–0.46
L(Se)Ge–Cl (VI)	0.69	0.69	sp ^{1.28} _(Ge) –sp ^{4.10} _(Cl)	1.48	–0.46
L(S)Ge–Br (6)	0.63	0.74	sp ^{4.35} _(Ge) –sp ^{5.09} _(Br)	1.51	–0.39
L(Se)Ge–Br (7)	0.64	0.74	sp ^{3.31} _(Ge) –sp ^{5.06} _(Br)	1.40	–0.39

^aL = (*t*-Bu)₂ATI (for compounds VII and VIII) and L = (*i*-Bu)₂ATI (for compounds V, VI, 6, and 7); X = F/Cl/Br; E = S/Se.

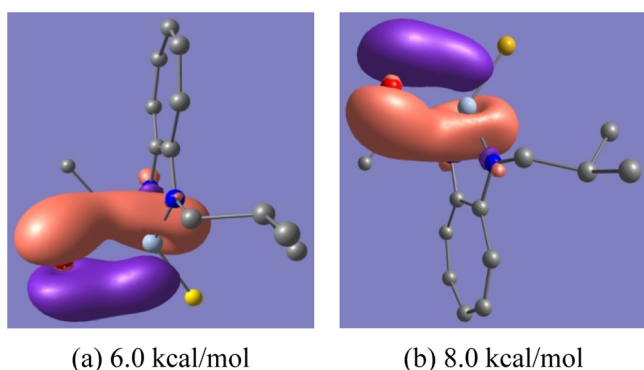


Figure 6. NBO interactions between the filled p-orbitals of bromine atoms and the vacant sp^x hybrid orbitals of germanium atoms in compounds 6 (*x* = 6.46, a) and 7 (*x* = 5.44, b).

Table 3. Computational Data for the Ge=E Bond in Compounds V–VIII, 6, and 7^a

compound	ionicity of the Ge=S/Se σ-bond	WBI of the Ge=S/Se bond	hybridization for the Ge=S/Se σ-bond	NPA charge on the
				S/Se atom
L(S)Ge–F (VII)	0.31	1.44	sp ^{0.45} _(Ge) –sp ^{6.51} _(S)	–0.80
L(Se)Ge–F (VIII)	0.08	1.48	sp ^{0.45} _(Ge) –sp ^{7.88} _(Se)	–0.69
L(S)Ge–Cl (V)	0.20	1.51	sp ^{0.97} _(Ge) –sp ^{6.56} _(S)	–0.73
L(Se)Ge–Cl (VI)	0.12	1.54	sp ^{1.25} _(Ge) –sp ^{7.96} _(Se)	–0.61
L(S)Ge–Br (6)	0.19	1.51	sp ^{0.67} _(Ge) –sp ^{6.62} _(S)	–0.72
L(Se)Ge–Br (7)	0.09	1.54	sp ^{0.74} _(Ge) –sp ^{8.02} _(Se)	–0.60

^aL = (*t*-Bu)₂ATI (for compounds VII and VIII) and L = (*i*-Bu)₂ATI (for compounds V, VI, 6, and 7)

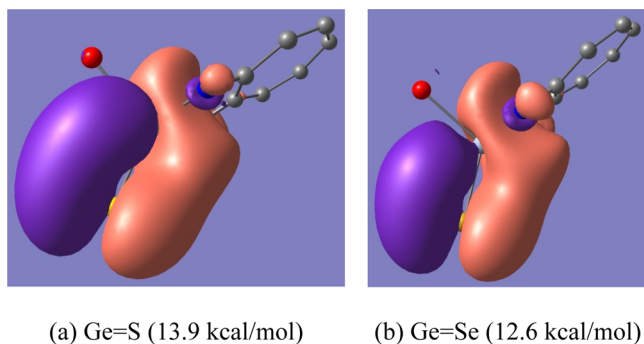


Figure 7. NBO pictures showing π-bonding interactions in (a) the Ge=S bond in compound 6 and (b) the Ge=Se bond in compound 7. Hydrogen atoms and isobutyl groups are omitted for clarity.

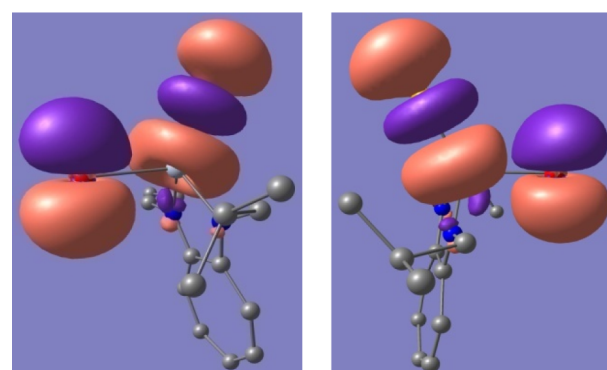


Figure 8. NBO interactions between the lone pairs of bromine atoms and the σ*-orbitals of the Ge–E bonds in compounds 6 and 7.

CONCLUSION

In summary, when the starting materials such as germylene monochloride **1** and germachalcogenoacid chlorides **V**/**VI** (with Ge–Cl bonds) failed to react with Me₃SiX (X = Br/CN), the utility of germylene amides (**2** and **2a**) and germaamides (**4**, **5**, **4a**, and **5a**) (with Ge–N bonds) as alternate precursors for the synthesis of other important germanium derivatives is demonstrated.

EXPERIMENTAL SECTION

All the reactions and handling of air- and moisture-sensitive compounds were carried out under a dry N₂ atmosphere using either standard Schlenk techniques or a glovebox equipped with a deep freezer. Solvents for the reactions and NMR spectroscopic studies were dried by following the standard procedures. Germylene monochloride **1**, *N*-germylenepyrrole **2a**, *N*-germathioacylpyrrole **4a**, and *N*-germaselenoacylpyrrole **5a** were prepared according to the reported procedures.^{3b,5b} LiN(SiMe₃)₂, sulfur, and selenium were purchased from Sigma-Aldrich. The obtained LiN(SiMe₃)₂ was purified by recrystallizing it in hexane. Trimethylsilyl bromide was purchased from Alfa Aesar and was purified by stirring it with excess of CaH₂ for 4 h followed by distillation. Trimethylsilyl cyanide was purchased from Spectrochem and was purified by distillation. Melting points of new compounds were recorded on a Unitech Sales digital melting point apparatus by sealing the compounds in glass capillaries. CHN elemental analyses were performed using a PerkinElmer CHN analyzer. ¹H, ¹³C, ²⁹Si, and ⁷⁷Se NMR spectra were recorded on a 300 MHz Bruker DPX-300 NMR spectrometer. The chemical shifts δ are reported in ppm and referenced internally with respect to residual solvent (¹H NMR) and solvent (¹³C NMR) resonances.¹⁷ For the ²⁹Si and ⁷⁷Se NMR spectroscopic studies (CH₃)₄Si and (CH₃)₂Se were used as the external references, respectively. The IR spectrum for compound **8** was recorded using an Agilent Resolutions Pro IR

spectrophotometer by keeping the sample inside a Harrick praying mantis ambient chamber. UV-vis spectra of compounds **3**, **6**, and **7** were recorded on a Shimadzu-UV-2600 UV-vis spectrophotometer at room temperature using screw-cap cuvettes.

Synthesis of [(i-Bu)₂ATiGe(SiMe₃)₂] (2). To a suspension of [(i-Bu)₂ATiGeCl] (**1**) (1.50 g, 4.42 mmol) in hexane (70 mL) was added LiN(SiMe₃)₂ (0.74 g, 4.42 mmol) at -40 °C, and the mixture stirred for 30 min. After that, the reaction mixture was brought to room temperature, stirred further for 12 h, and filtered through a G4 frit. Removal of all the volatiles from the filtrate under reduced pressure gave compound **2** as a dark red solid. Yield: 1.97 g (4.24 mmol), 96.0%. Mp: 72 °C. Anal. Calcd for C₂₁H₄₁GeN₃Si₂ (*M* = 465.21): C, 54.31; H, 8.90; N, 9.05. Found: C, 54.35; H, 8.83; N, 9.11. ¹H NMR (300 MHz, C₆D₆): δ 0.36 (s, 18H, Si(CH₃)₃), 0.81 (d, ³J_{HH} = 6.9 Hz, 6H, CH(CH₃)₂), 1.00 (d, ³J_{HH} = 6.6 Hz, 6H, CH(CH₃)₂), 2.05–2.18 (m, 2H, CH(CH₃)₃), 3.07 (dd, *J*_{HH} = 13.8, 5.7 Hz, 2H, CH₂), 3.27 (dd, *J*_{HH} = 13.8, 8.7 Hz, 2H, CH₂), 6.05 (t, ³J_{HH} = 9.3 Hz, 1H, CH), 6.14 (d, ³J_{HH} = 11.4 Hz, 2H, CH), 6.63 (dd, ³J_{HH} = 11.7, 9.9 Hz, 2H, CH). ¹³C{¹H} NMR (75 MHz, C₆D₆): δ 5.93 (Si(CH₃)₃), 21.27 (CH(CH₃)₂), 21.55 (CH(CH₃)₂), 27.63 (CH(CH₃)₂), 54.43 (CH₂), 114.47 (C₄), 119.26 (C_{2,6}), 136.84 (C_{3,5}), 161.37 (C_{1,7}). ²⁹Si{¹H} NMR (60 MHz, C₆D₆): δ -0.93 (Si(CH₃)₃).

Synthesis of [(i-Bu)₂ATiGeBr] (3). To a solution of compound **2** (0.15 g, 0.32 mmol) in tetrahydrofuran (20 mL) was added Me₃SiBr (0.25 g, 1.63 mmol) at room temperature, and the mixture stirred for 2 h. Then, all the volatiles were removed under reduced pressure. The obtained residue was washed with cold hexane (5 mL) and dried *in vacuo* to afford an analytically pure sample of compound **3** as an orange solid. Single crystals of compound **3** suitable for X-ray diffraction studies were obtained by cooling its tetrahydrofuran solution at -40 °C. Yield: 0.12 g (0.31 mmol), 96.8%. Mp: 110 °C. Anal. Calcd for C₁₅H₂₃BrGeN₂ (*M* = 384.03): C, 46.93; H, 6.04; N, 7.30. Found: C, 46.87; H, 6.13; N, 7.35. ¹H NMR (300 MHz, CDCl₃): δ 1.05 (d, ³J_{HH} = 6.3 Hz, 12H, CH(CH₃)₂), 2.20–2.33 (m, 2H, CH(CH₃)₃), 3.56 (d, ³J_{HH} = 7.2 Hz, 4H, CH₂), 6.83 (t, ³J_{HH} = 9.3 Hz, 1H, CH), 6.93 (d, ³J_{HH} = 11.1 Hz, 2H, CH), 7.34 (t, ³J_{HH} = 10.5 Hz, 2H, CH). ¹³C{¹H} NMR (75 MHz, CDCl₃): δ 21.27 (CH(CH₃)₂), 28.06 (CH(CH₃)₂), 54.19 (CH₂), 116.93 (C₄), 124.29 (C_{2,6}), 137.03 (C_{3,5}), 161.25 (C_{1,7}). UV-vis (THF) λ_{max}/nm (ε/M⁻¹cm⁻¹): 267 (35 868), 360 (15 689), 418 (10 240), 427 (10 659).

Synthesis of [(i-Bu)₂ATiGe(SiN(SiMe₃)₂)] (4). To a solution of compound **2** (0.40 g, 0.86 mmol) in tetrahydrofuran (20 mL) was added elemental sulfur (0.03 g, 0.86 mmol) at room temperature, and the mixture stirred for 3 h. Then, all the volatiles were removed under reduced pressure. The obtained residue was washed with hexane (5 mL) and dried *in vacuo* to obtain compound **4** as a yellow solid. Single crystals of compound **4** suitable for X-ray diffraction studies were obtained by cooling its tetrahydrofuran solution at -40 °C. Yield: 0.42 g (0.85 mmol), 98.2%. Mp: 191 °C (dec). Anal. Calcd for C₂₁H₄₁GeN₃SSi₂ (*M* = 497.18): C, 50.81; H, 8.32; N, 8.46. Found: C, 50.87; H, 8.37; N, 8.39. ¹H NMR (300 MHz, CDCl₃): δ 0.24 (s, 18H, Si(CH₃)₃), 1.07 (d, ³J_{HH} = 6.9 Hz, 6H, CH(CH₃)₂), 1.11 (d, ³J_{HH} = 6.6 Hz, 6H, CH(CH₃)₂), 2.38–2.51 (m, 2H, CH(CH₃)₂), 3.44 (dd, *J*_{HH} = 13.8, 7.2 Hz, 2H, CH₂), 3.71 (dd, *J*_{HH} = 13.8, 6.6 Hz, 2H, CH₂), 6.78 (t, ³J_{HH} = 9.3 Hz, 1H, CH), 6.91 (d, ³J_{HH} = 11.1 Hz, 2H, CH), 7.34 (t, ³J_{HH} = 10.2 Hz, 2H, CH). ¹³C{¹H} NMR (75 MHz, CDCl₃): δ 5.78 (Si(CH₃)₃), 21.64 (CH(CH₃)₂), 21.94 (CH(CH₃)₂), 28.83 (CH(CH₃)₂), 53.88 (CH₂), 116.54 (C₄), 124.64 (C_{2,6}), 138.36 (C_{3,5}), 157.53 (C_{1,7}). ²⁹Si{¹H} NMR (60 MHz, CDCl₃): δ 5.36 (Si(CH₃)₃).

Synthesis of [(i-Bu)₂ATiGe(S)Br] (6). To a solution of compound **4** (0.30 g, 0.60 mmol) in tetrahydrofuran (50 mL) was added Me₃SiBr (0.93 g, 6.04 mmol) at room temperature, and the mixture refluxed for 18 h. Then, all the volatiles were removed under reduced pressure. The obtained residue was washed with hexane (7 mL) and dried *in vacuo* to afford an analytically pure sample of compound **6** as a yellow solid. Single crystals of compound **6** suitable for X-ray diffraction studies were obtained by slow evaporation of its tetrahydrofuran solution at room temperature. Yield: 0.23 g (0.55 mmol), 91.4%. Mp: 119 °C. Anal. Calcd for C₁₅H₂₃BrGeN₂S (*M* = 416.00): C, 43.31; H,

5.57; N, 6.73. Found: C, 43.22; H, 5.50; N, 6.81. ¹H NMR (300 MHz, CDCl₃): δ 1.06 (d, ³J_{HH} = 6.3 Hz, 12H, CH(CH₃)₂), 2.36–2.50 (m, 2H, CH(CH₃)₃), 3.62 (dd, *J*_{HH} = 14.1, 8.4 Hz, 2H, CH₂), 3.78 (dd, *J*_{HH} = 14.1, 6.6 Hz, 2H, CH₂), 7.07 (t, ³J_{HH} = 9.6 Hz, 1H, CH), 7.15 (d, ³J_{HH} = 11.4 Hz, 2H, CH), 7.56 (t, ³J_{HH} = 10.5 Hz, 2H, CH). ¹³C{¹H} NMR (75 MHz, CDCl₃): δ 20.01 (CH(CH₃)₂), 20.10 (CH(CH₃)₂), 27.03 (CH(CH₃)₂), 52.36 (CH₂), 116.83 (C₄), 126.35 (C_{2,6}), 138.05 (C_{3,5}), 155.46 (C_{1,7}). UV-vis (THF) λ_{max}/nm (ε/M⁻¹cm⁻¹): 268 (37 844), 362 (15 210), 435 (9 581).

Synthesis of [(i-Bu)₂ATiGe(S)Br] (6) from Compound 3. To a solution of compound **3** (0.36 g, 0.94 mmol) in tetrahydrofuran (30 mL) was added elemental sulfur (0.03 g, 0.94 mmol) at room temperature, and the mixture stirred for 12 h. Then, all the volatiles were removed under reduced pressure. The obtained residue was washed with hexane (3 mL) and dried *in vacuo* to obtain compound **6** as a yellow solid. Yield: 0.35 g (0.84 mmol), 90.0%.

Synthesis of [(i-Bu)₂ATiGe(Se)Br] (7) from Compound 3. To a solution of compound **3** (0.34 g, 0.89 mmol) in tetrahydrofuran (25 mL) was added selenium powder (0.08 g, 1.06 mmol) at room temperature, and the mixture stirred for 36 h. Then, the reaction mixture was filtered through a G4 frit with Celite, and all the volatiles from the filtrate were removed under reduced pressure. The obtained residue was washed with hexane (4 mL) and dried *in vacuo* to obtain compound **7** as an orange solid. Yield: 0.34 g (0.74 mmol) 83.0% (for characterization see the [Supporting Information](#)).

Synthesis of [(i-Bu)₂ATiGeCN] (8). To a solution of N-germylenepyrrole **2a** (0.50 g, 1.37 mmol) in tetrahydrofuran (10 mL) was added Me₃SiCN (1.34 g, 13.51 mmol) at room temperature, and the mixture stirred for 12 h. All the volatiles were then removed under reduced pressure. The obtained residue was washed with cold hexane (5 mL) and dried *in vacuo* to afford an analytically pure sample of compound **8** as an orange solid. Single crystals of compound **8** suitable for X-ray diffraction studies were obtained by cooling its tetrahydrofuran solution at -40 °C. Yield: 0.43 g (1.30 mmol), 96.2%. Mp: 109 °C. Anal. Calcd for C₁₆H₂₃GeN₃ (*M* = 330.01): C, 58.23; H, 7.02; N, 12.73. Found: C, 58.21; H, 6.97; N, 12.77. ¹H NMR (300 MHz, CDCl₃): δ 1.04 (d, ³J_{HH} = 6.0 Hz, 12H, CH(CH₃)₂), 2.12–2.26 (m, 2H, CH(CH₃)₂), 3.29 (dd, *J*_{HH} = 13.8, 7.8 Hz, 2H, CH₂), 3.40 (dd, *J*_{HH} = 13.8, 6.6 Hz, 2H, CH₂), 6.58 (t, ³J_{HH} = 9.6 Hz, 1H, CH), 6.65 (d, ³J_{HH} = 11.4 Hz, 2H, CH), 7.18 (t, ³J_{HH} = 10.5 Hz, 2H, CH). ¹³C{¹H} NMR (75 MHz, CDCl₃): δ 21.17 (CH(CH₃)₂), 21.24 (CH(CH₃)₂), 28.30 (CH(CH₃)₂), 54.58 (CH₂), 115.78 (C₄), 122.37 (C_{2,6}), 137.48 (CN), 137.65 (C_{3,5}), 162.80 (C_{1,7}). IR (KBr): $\tilde{\nu}$ = 2123.83 cm⁻¹ (C≡N).

X-ray Structure Determination for Compounds 3–8 and VII.

The X-ray data for compounds **3–8** and **VII** were collected using a Bruker SMART APEX diffractometer equipped with a 3-axis goniometer¹⁸ at either room temperature (298 K) (for compounds **3–5** and **VII**), or 100 K (for compounds **6** and **7**), 150 K (for compound **8**) (Table S1, see the [Supporting Information](#)). The crystals were covered with a cryoprotectant and then mounted on a glass fiber. SAINT and SADABS were used to integrate the data and apply an empirical absorption correction, respectively.¹⁹ SHELXTL was used for the structural solution by direct methods and refinement by full matrix least-squares on *F*².²⁰ Anisotropic refinement was performed for all the non-hydrogen atoms. A riding model was used to fix the positions of the hydrogen atoms, and the hydrogen atoms were refined isotropically. The important crystallographic data for compounds **3–8** and **VII** are given in Table S1 (see the [Supporting Information](#)).

Computational Details. GAUSSIAN-09 programs were used for carrying out all the theoretical calculations.¹⁴ The B3LYP level of theory was used for optimizing the geometries of compounds **1**, **2**, **6**, **7**, and **V–VIII** using LANL2DZ (having ECP for core electrons) (for sulfur, selenium, and germanium atoms) and 6-31+G** (for the rest of the elements) basis sets. For geometry optimizations, the coordinates obtained from single-crystal X-ray diffraction studies were used.^{3b,6,21} The frequency calculations were carried out for all the optimized geometries of compounds **1**, **2**, **6**, **7**, and **V–VIII** to characterize the stationary points as minima. The same level of theory, basis sets, and

the optimized coordinates were used for performing molecular orbital calculations, Weinhold's natural bond orbital,^{15,16} NPA charges, and WBI analyses on these compounds. Chemcraft software (<http://www.chemcraftprog.com>) was used for plotting the NBO interactions. To explain the UV-vis spectra of compounds **3**, **6**, and **7**, TDDFT-PCM calculations were carried out on these compounds using optimized coordinates and tetrahydrofuran as the solvent at the aforementioned level of theory and basis sets. For BDE calculations, LGe[•], Cl[•], and [•]N(TMS)₂ were modeled through the Chemcraft software by omitting the Cl[•] from compound **1** and [•]N(TMS)₂ from compound **2** and optimized at the aforementioned level of theory and basis sets.

■ ASSOCIATED CONTENT

📄 Supporting Information

The Supporting Information is available free of charge on the ACS Publications website at DOI: 10.1021/acs.organomet.5b00643.

Crystallographic information files for compounds **3–8** and **VII** (CIF)

Synthesis of compounds **5** and **7**, alternative synthetic routes for compounds **3**, **6**, and **7**, variable-temperature ¹H NMR spectra of compound **2** (Figure S1), crystal data and structure refinement parameters for compounds **3–8** and **VII** (Table S1), DFT-computed bond dissociation enthalpies of Ge–Cl bonds in compounds **1**, **V**, and **VI** and Ge–N bonds in compounds **2**, **4**, and **5** (Table S2), molecular structure of germathioamide **4** (Figure S2), molecular structure of germaselenoacid bromide **7** (Figure S3), NBO interactions between the filled orbitals of halogen atoms (X) and the vacant orbitals of germanium atoms in compounds **V** and **VI** (X = Cl; Figures a,b) and **VII** and **VIII** (X = F; Figures c–l) (Figure S4), molecular structure of germathioacid fluoride **VII** (Figure S5), complete author list for ref 14 (PDF)

■ AUTHOR INFORMATION

Corresponding Author

*Phone: +91-11-2659 1523. Fax: +91-11-2658 1102. E-mail: sisn@chemistry.iitd.ac.in.

Notes

The authors declare no competing financial interest.

■ ACKNOWLEDGMENTS

R.K.S. and S.K. thank the Council of Scientific and Industrial Research (CSIR), New Delhi, India, for Senior Research Fellowships (SRF). M.K.S. thanks IIT Delhi, New Delhi, India, for the SRF. S.N. thanks the Department of Science and Technology (DST), New Delhi, India, for financial support (SB/S1/IC-46/2013). S.N. also thanks the DST-FIST for providing financial assistance to the Department of Chemistry, IIT Delhi, New Delhi, India, to establish several important research facilities such as single-crystal X-ray diffraction and HRMS. Dedicated to Prof. Maravanji S Balakrishna.

■ REFERENCES

(1) (a) Prabusankar, G.; Sathyanarayana, A.; Suresh, P.; Babu, C. N.; Srinivas, K.; Metla, B. P. R. *Coord. Chem. Rev.* **2014**, *269*, 96. (b) Asay, M.; Jones, C.; Driess, M. *Chem. Rev.* **2011**, *111*, 354. (c) Fischer, R. C.; Power, P. P. *Chem. Rev.* **2010**, *110*, 3877. (d) Mandal, S. K.; Roesky, H. W. *Chem. Commun.* **2010**, *46*, 6016. (e) Lee, V. Y.; Sekiguchi, A. *Organometallic Compounds of Low-Coordinate Si, Ge, Sn, and Pb: From Phantom Species to Stable Compounds*; Wiley: Chichester, U.K., 2010.

(f) Mizuhata, Y.; Sasamori, T.; Tokitoh, N. *Chem. Rev.* **2009**, *109*, 3479. (g) Nagendran, S.; Roesky, H. W. *Organometallics* **2008**, *27*, 457. (h) Zabula, A. V.; Hahn, F. E. *Eur. J. Inorg. Chem.* **2008**, *2008*, 5165. (i) Leung, W.-P.; Kan, K.-W.; Chong, K.-H. *Coord. Chem. Rev.* **2007**, *251*, 2253. (j) Saur, I.; Alonso, S. G.; Barrau, J. *Appl. Organomet. Chem.* **2005**, *19*, 414. (k) Kühn, O. *Coord. Chem. Rev.* **2004**, *248*, 411. (l) Bourget-Merle, L.; Lappert, M. F.; Severn, J. R. *Chem. Rev.* **2002**, *102*, 3031. (m) Tokitoh, N.; Okazaki, R. *Coord. Chem. Rev.* **2000**, *210*, 251. (n) Weidenbruch, M. *Eur. J. Inorg. Chem.* **1999**, *1999*, 373. (o) Barrau, J.; Rima, G. *Coord. Chem. Rev.* **1998**, *178–180*, 593. (p) Neumann, W. P. *Chem. Rev.* **1991**, *91*, 311. (2) (a) Fjeldberg, T.; Haaland, A.; Schilling, B. E. R.; Lappert, M. F.; Thorne, A. J. *J. Chem. Soc., Dalton Trans.* **1986**, 1551. (b) Satgé, J.; Massol, M.; Rivière, P. J. *Organomet. Chem.* **1973**, *56*, 1. (c) Kulishov, V. I.; Bokii, N. G.; Struchkov, Y. T.; Nefedov, O. M.; Kolesnikov, S. P.; Perlmutter, B. L. *J. Struct. Chem.* **1970**, *11*, 61. (d) Kolesnikov, S. P.; Shiryayev, V. I.; Nefedov, O. M. *Izv. Akad. Nauk SSSR, Ser. Khim.* **1966**, 584. (3) (a) Jha, C. K.; Karwasara, S.; Nagendran, S. *Chem. - Eur. J.* **2014**, *20*, 10240. (b) Sinhababu, S.; Siwatch, R. K.; Mukherjee, G.; Rajaraman, G.; Nagendran, S. *Inorg. Chem.* **2012**, *51*, 9240. (c) Ding, Y.; Hao, H.; Roesky, H. W.; Noltemeyer, M.; Schmidt, H.-G. *Organometallics* **2001**, *20*, 4806. Also, see ref 4d. (4) (a) Matioszek, D.; Katir, N.; Saffon, N.; Castel, A. *Organometallics* **2010**, *29*, 3039. (b) Jana, A.; Schwab, G.; Roesky, H. W.; Stalke, D. *Inorg. Chim. Acta* **2010**, *363*, 4408. (c) Ruddy, A. J.; Rupar, P. A.; Bladek, K. J.; Allan, C. J.; Avery, J. C.; Baines, K. M. *Organometallics* **2010**, *29*, 1362. (d) Rupar, P. A.; Jennings, M. C.; Baines, K. M. *Organometallics* **2008**, *27*, 5043. (e) Driess, M.; Yao, S.; Brym, M.; van Wüllen, C. *Angew. Chem., Int. Ed.* **2006**, *45*, 4349. (f) Meller, M.; Gräbe, C.-P. *Chem. Ber.* **1985**, *118*, 2020. (5) (a) Rupar, P. A.; Staroverov, V. N.; Ragogna, P. J.; Baines, K. M. *J. Am. Chem. Soc.* **2007**, *129*, 15138. (b) Akkari, A.; Byrne, J. J.; Saur, I.; Rima, G.; Gornitzka, H.; Barrau, J. *J. Organomet. Chem.* **2001**, *622*, 190. (c) Arduengo, A. J., III; Dias, H. V. R.; Calabrese, J. C.; Davidson, F. *Inorg. Chem.* **1993**, *32*, 1541. (d) Stobart, S. R. *J. Chem. Soc., Chem. Commun.* **1979**, 911. Also, see ref 4c. (6) (a) Siwatch, R. K.; Yadav, D.; Mukherjee, G.; Rajaraman, G.; Nagendran, S. *Inorg. Chem.* **2014**, *53*, 5073. (b) Karwasara, S.; Sharma, M. K.; Tripathi, R.; Nagendran, S. *Organometallics* **2013**, *32*, 3830. (7) (a) Izod, K.; Stewart, J.; Clark, E. R.; McFarlane, W.; Allen, B.; Clegg, W.; Harrington, R. W. *Organometallics* **2009**, *28*, 3327. (b) Izod, K.; McFarlane, W.; Allen, B.; Clegg, W.; Harrington, R. W. *Organometallics* **2005**, *24*, 2157. (8) Siwatch, R. K.; Nagendran, S. *Chem. - Eur. J.* **2014**, *20*, 13551. (9) (a) Yadav, D.; Siwatch, R. K.; Mukherjee, G.; Rajaraman, G.; Nagendran, S. *Inorg. Chem.* **2014**, *53*, 10054. (b) Siwatch, R. K.; Nagendran, S. *Organometallics* **2012**, *31*, 3389. (c) Siwatch, R. K.; Yadav, D.; Mukherjee, G.; Rajaraman, G.; Nagendran, S. *Inorg. Chem.* **2013**, *52*, 13384. (10) (a) Leung, W.-P.; Chiu, W.-K.; Chong, K.-H.; Mak, T. C. W. *Chem. Commun.* **2009**, 6822. (b) Foley, S. R.; Bensimon, C.; Richeson, D. S. *J. Am. Chem. Soc.* **1997**, *119*, 10359. (c) Veith, M.; Rammo, A. Z. *Anorg. Allg. Chem.* **1997**, *623*, 861. (d) Veith, M.; Becker, S.; Huch, V. *Angew. Chem., Int. Ed. Engl.* **1989**, *28*, 1237. (e) Karwasara, S.; Siwatch, R. K.; Jha, C. K.; Nagendran, S. *Organometallics* **2015**, *34*, 3246. (11) (a) Leung, W.-P.; Chong, K.-H.; Wu, Y.-S.; So, C.-W.; Chan, H.-S.; Mak, T. C. W. *Eur. J. Inorg. Chem.* **2006**, *2006*, 808. (b) Ding, Y.; Ma, Q.; Roesky, H. W.; Usón, I.; Noltemeyer, I.; Schmidt, H.-G. *Dalton Trans.* **2003**, 1094. (c) Saur, I.; Rima, G.; Gornitzka, H.; Miqueu, K.; Barrau, J. *Organometallics* **2003**, *22*, 1106. (d) Ding, Y.; Ma, Q.; Usón, I.; Roesky, H. W.; Noltemeyer, M.; Schmidt, H.-G. *J. Am. Chem. Soc.* **2002**, *124*, 8542. (e) Karwasara, S.; Yadav, D.; Jha, C. K.; Rajaraman, G.; Nagendran, S. *Chem. Commun.* **2015**, *51*, 4310. (12) (a) Matsumoto, T.; Tokitoh, N.; Okazaki, R. *J. Am. Chem. Soc.* **1999**, *121*, 8811. (b) Matsumoto, T.; Tokitoh, N.; Okazaki, R. *Angew. Chem., Int. Ed. Engl.* **1994**, *33*, 2316. (c) Tokitoh, N.; Matsumoto, T.; Manmaru, K.; Okazaki, R. *J. Am. Chem. Soc.* **1993**, *115*, 8855.

- (13) Walding, J. L.; Fanwick, P. E.; Weinert, C. S. *Inorg. Chim. Acta* **2005**, *358*, 1186.
- (14) Frisch, M. J.; et al. *Gaussian 09*, Revision C. 01; Gaussian, Inc.: Wallingford, CT, 2010.
- (15) Weinhold, F.; Landis, C. R. *Valency and Bonding*; Cambridge: Cambridge, U.K., 2005.
- (16) (a) Reed, A. E.; Curtiss, L. A.; Weinhold, F. *Chem. Rev.* **1988**, *88*, 899. (b) Glendening, E. D.; Reed, A. E.; Carpenter, J. E.; Weinhold, F. *NBO*, Version 3.1; Theoretical Chemistry Institute, University of Wisconsin: Madison WI, 1996.
- (17) Fulmer, G. R.; Miller, A. J. M.; Sherden, N. H.; Gottlieb, H. E.; Nudelman, A.; Stoltz, B. M.; Bercaw, J. E.; Goldberg, K. I. *Organometallics* **2010**, *29*, 2176.
- (18) *SMART: Bruker Molecular Analysis Research Tool*, Version 5.618; Bruker AXS: Madison, WI, 2000.
- (19) *SAINT-NT*, Version 6.04; Bruker AXS: Madison, WI, 2001.
- (20) *SHELXTL-NT*, Version 6.10; Bruker AXS: Madison, WI, 2000.
- (21) The synthesis of germathioacid fluoride [(*i*-Bu)₂ATiGe(S)F] (**VII**) was reported earlier (see ref **3b**). For theoretical calculations, the structural study was performed and reported as [Figure S5](#).